

Diagnosing Harmful Continuation in Answer-Correct Long-CoT Training Traces

Chen He^{1*} Yuhao Wu^{2*} Lei Wang³ Wenxuan Zhang² Fumin Shen^{1†}

¹University of Electronic Science and Technology of China

²Singapore University of Technology and Design ³Singapore Management University

*Equal contribution † Corresponding author

Abstract

Long chain-of-thought (CoT) traces are widely used as supervision for reasoning-oriented LLM SFT, yet answer-correct traces can still lead to markedly different fine-tuning outcomes. We study post-conclusion continuation in answer-correct long-CoT data: a continuation where the answer appears sufficiently supported, but the trace continues with additional reasoning that remains in the supervised target. To test its training effect, we use a delete-only editor to construct answer-preserving suffix removal and compare CoT-based SFT on the original and processed traces. We observe improved SFT outcomes after removing the editor-identified post-conclusion continuation, suggesting that this continuation is harmful to training in our setting. We therefore refer to this empirically supported phenomenon as *harmful continuation*. Beyond this intervention, we further characterize the removed post-conclusion continuation through uncertainty and hidden-state progress. We observe persistent local uncertainty together with weakened terminal-directional progress, forming an uncertainty–geometry mismatch. Finally, we instantiate *Harmful Continuation Cut (HCC)*, a lightweight boundary proxy that approximates the editor-identified post-conclusion continuation boundary.

1 Introduction

Long chain-of-thought traces have become important training targets for reasoning models (Wei et al., 2022; Luo et al., 2025b; Ou and Yin, 2025). They are used not only in supervised fine-tuning (Ou and Yin, 2025), but also in reasoning-oriented continued training and as cold-start data before reinforcement learning (Wang et al., 2026). Unlike final-answer annotations, long-CoT traces expose full reasoning trajectories that models are encouraged to imitate during training. This makes CoT trace quality a central issue for reasoning training

where the training target specifies not only what answer to produce, but also what trajectory should be treated as learnable reasoning behavior.

Prior work has already shown that answer-correct CoT traces can differ substantially in training utility. The style and structure of source trajectories can affect the generalization of SFT models (Tian et al., 2025; Zhang et al., 2025; Li et al., 2025), and recent studies further connect trace compatibility, reasoning patterns, and learnability to downstream outcomes (Liu et al., 2026; Li et al., 2026). However, most existing methods remain confined to trace selection, prefix selection, or externally guided rewriting, which leaves the internal failure mode of answer-correct traces underexplained. As a result, they do not characterize where useful reasoning may end and begin, or why such a phase can be associated with weaker SFT despite preserving answer correctness.

To address this gap, we take a diagnostic view of answer-correct long-CoT traces. We seek a trace-internal diagnostic explanation for why answer-correct traces may differ in training utility, rather than assuming that a long reasoning trace is uniformly useful once its final answer is correct. Our goal is not to claim that every long tail is harmful, nor to treat length as the central issue. Instead, we ask whether some traces enter a low-value post-conclusion continuation: the answer is already sufficiently supported, but subsequent reasoning remains locally costly while showing weak hidden-state progress. From the uncertainty perspective, we observe that some post-conclusion continuation remains locally costly or unstable, suggesting that the trace continues to explore after evaluator-based answer support has largely saturated. From the geometric perspective, this continued exploration shows weakened terminal-directional hidden-state progress. We refer to this hypothesized low-value phase as post-conclusion continuation before evaluating its downstream training effect. When answer-

preserving removal of this continuation improves SFT outcomes, we call the empirically supported training-unfavorable case harmful continuation.

To examine the training relevance of this post-conclusion continuation, we use a delete-only editor as an operational intervention tool. The editor does not rewrite the trace; it only removes post-conclusion suffixes while preserving the original prefix and final answer. This allows us to test whether answer-preserving removal of the post-conclusion continuation improves SFT outcomes. Motivated by this diagnosis, we instantiate *Harmful Continuation Cut (HCC)*, a lightweight boundary proxy. HCC uses a frozen Qwen2.5-0.5B-Instruct backbone with a cut head to extract sentence-level reasoning states and approximate the editor-identified post-conclusion continuation.

Our contributions can be summarized as follows:

- We formulate post-conclusion continuation in answer-correct long-CoT traces without assuming inherent harmfulness.
- We show through answer-preserving suffix removal that the removed continuation is training-unfavorable in our SFT settings.
- We characterize the removed continuation with an uncertainty–geometry mismatch and propose HCC as a proxy to remove it.

2 Related Work

Long-CoT reasoning training. Long-CoT traces have become important for post-training pipelines. While early pipelines often treat answer-correct traces as directly usable supervision, recent studies show that correctness alone does not determine their training value. Work on data selection, trace compatibility, and informative alignment (Yang et al., 2026; Zhang et al., 2025; Chandra et al., 2025) suggests that only a subset of answer-correct traces provides beneficial supervision. Other approaches modify or shorten reasoning traces through sequence truncation, prefix optimization, adaptive prefix alignment, robustness to partial reasoning, or length-aware training (Chen et al., 2025a; Sun et al., 2026; Liu et al., 2026; Silvestri and Cetin, 2026; Xu et al., 2025; Luo et al., 2025a; Ma et al., 2025). However, these methods mainly operate in a heuristic manner. They do not directly characterize where useful reasoning may end, where useless reasoning may begin, or why

this reasoning can be associated with weaker SFT supervision despite answer correctness.

Properties of long-CoT trajectories. Recent work increasingly treats long-CoT traces as structured reasoning trajectories rather than flat text sequences. Studies on overthinking show that long-reasoning models may repeatedly verify intermediate conclusions or continue reasoning without meaningful gain (Chen et al., 2025b). Complementary analyses examine global reasoning patterns, trajectory geometry, and step-level anchors that contribute to actual progress (Jiang et al., 2025; Ballon et al., 2026; Bogdan et al.; Yang et al., 2025). Most closely related to our motivation, Li et al. (2026) connects trajectory properties to downstream SFT outcomes and shows that different reasoning patterns can lead to different generalization behavior. Our work builds on this trajectory-level view, but focuses on a post-conclusion continuation inside answer-correct traces: continuation that remains uncertain or costly while showing weakened terminal-directional progress.

3 Operational Partition and Diagnostics of Post-Conclusion Continuation

3.1 Data Construction

In this section, we do not assume that editor-removed sentences are ground-truth harmful continuation. Instead, we use the delete-only editor to construct an operational partition for diagnosing post-conclusion suffixes. The resulting groups are used to reveal statistical signatures of a possible low-value phase, rather than to define harmfulness by editor decisions alone. We use Qwen3-235B-A22B-Instruct-2507 (Team, 2025) and DeepSeek-R1-V3.2 (Guo et al., 2025) to generate trajectories, and sample 4,780 answer-correct long-CoT solution trajectories from the OpenR1-Math-220k dataset. These trajectories serve as the original CoT training traces. For simplicity, we use $\{T\}_Q$ and $\{T\}_R$ to refer to the two sets of trajectories from the two models, respectively. We then employ Qwen3.5-27B (Team, 2025) as a delete-only offline editor to expose post-conclusion continuation for empirical analysis. Given a trajectory from $\{T\}_Q$ or $\{T\}_R$, the editor marks the post-conclusion sentences that can be removed while preserving the reasoning necessary to recover the final answer.

Operational groups. We divide each edited trajectory into two operational groups. The first

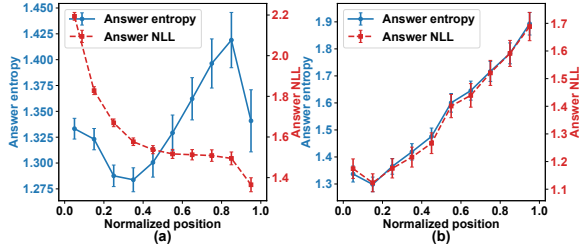


Figure 1: Evaluator-based uncertainty diagnostics as reasoning segments are progressively added for (a) retained reasoning and (b) editor-removed continuation.

group is the *retained reasoning*, namely the editor-preserved portion that supports the final answer. The second group is the *editor-removed continuation*, namely the post-conclusion continuation marked as removable by the offline editor. At this stage, these terms refer to operational groups rather than predefined theoretical labels.

3.2 Uncertainty View

In this section, we aim to answer the following question: *Does the post-conclusion continuation continue to improve evaluator-based final-answer recoverability, or does answer support appear to saturate while local uncertainty remains high?*

Comparison protocols. We analyze uncertainty at both answer and sentence levels. At the answer level, we progressively append reasoning sentences along the same complete response trajectory and compute prefix-conditioned final-answer entropy and NLL. These quantities should be interpreted as evaluator-based diagnostics of answer recoverability, rather than direct measurements of causal reasoning contribution. For segment-wise visualization, positions are normalized separately within retained reasoning and the subsequent editor-removed continuation. At the sentence level, we use sentence entropy and sentence NLL to measure local predictive difficulty. For boundary-level analysis, we track K_1 , K_T , C_1 , and C_T , denoting the first and last sentences of retained reasoning and editor-removed continuation, and compare both local uncertainty changes and answer-NLL reduction. The detailed protocols are described in the Appendix.

Answer uncertainty dynamics. Figure 1 shows how answer-level uncertainty changes as reasoning sentences are progressively appended to the same complete response. For visualization, the x-axis is normalized within its corresponding segment, with Figure 1 (a) showing retained reasoning and Figure 1 (b) showing the subsequent editor-removed

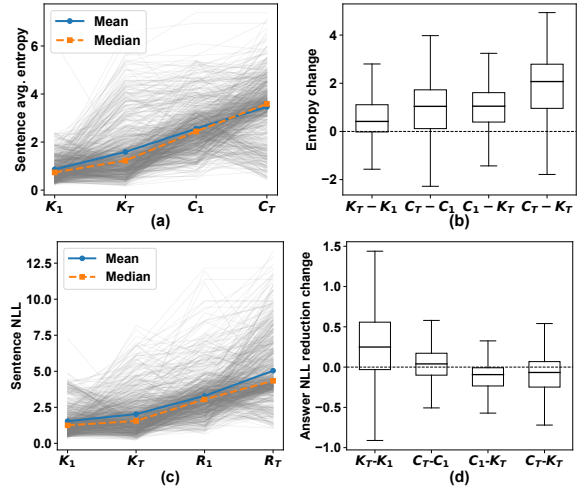


Figure 2: Boundary-level diagnostic changes around the editor-identified post-conclusion continuation: (a) sentence entropy, (b) entropy change, (c) sentence NLL, and (d) answer-NLL reduction change.

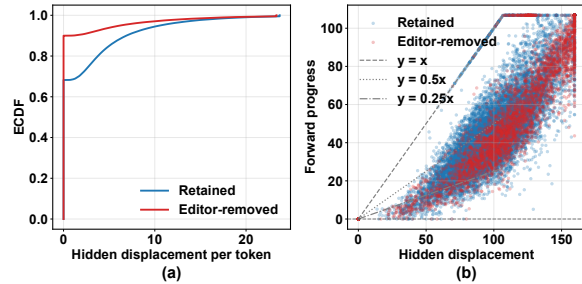


Figure 3: Operational hidden-state progress of retained reasoning and editor-removed continuation: (a) ECDF of token-normalized hidden displacement and (b) hidden displacement versus forward progress.

continuation. In retained reasoning, answer entropy changes non-monotonically but does not exhibit a persistent increase, while answer NLL steadily decreases as more useful reasoning is added. This suggests that the retained segment improves evaluator-based final-answer recoverability even when intermediate reasoning involves local exploration or verification. In contrast, once the trace enters editor-removed continuation, both answer entropy and answer NLL increase as more post-conclusion content is appended. This suggests that the continuation does not consistently improve evaluator-based answer recoverability, but instead introduces a higher-uncertainty state after the answer has been sufficiently supported.

Boundary-level mismatch. Figure 2 examines local uncertainty and evaluator-based answer-support changes on the boundary between retained reasoning and editor-removed continuation. From K_1 to K_T , sentence entropy and sentence NLL increase, but the answer-NLL reduction also be-

Table 1: Paired per-sample comparison of operational hidden-state progress between editor-removed continuation and retained reasoning. The paired difference is defined as $\Delta = \text{Removed mean} - \text{Retained mean}$.

Metric	Removed mean	Retained mean	Removed lower	Removed higher	95% CI of Δ
Hidden displacement	21.91	44.92	0.79	0.16	$[-23.85, -22.19]$
Forward progress	10.79	20.50	0.79	0.17	$[-10.15, -9.31]$
Progress efficiency	0.09	0.19	0.79	0.17	$[-0.11, -0.10]$
Hidden displacement / token	1.65	2.83	0.79	0.16	$[-1.24, -1.11]$
Forward progress / token	0.84	1.28	0.79	0.17	$[-0.47, -0.40]$
Curvature	1.09	1.17	0.73	0.27	$[-0.09, -0.08]$

comes stronger, suggesting that local uncertainty within retained reasoning can still accompany improved answer recoverability under the evaluator. The transition from K_T to C_1 shows a different pattern. Local uncertainty rises at the beginning of editor-removed continuation, while the gain in answer support no longer increases correspondingly. From C_1 to C_T , this high-uncertainty regime is maintained or amplified, but the continuation does not provide stable additional answer-NLL reduction. The candidate low-value pattern therefore emerges when increased local prediction difficulty is no longer matched by consistent improvements in evaluator-based final-answer recoverability.

3.3 Geometric View

Following the uncertainty analysis, another question arises: *Does the increased predictive uncertainty of post-conclusion continuation translate into effective hidden-state progress?*

Comparison protocols. Following prior work on the geometry of Transformer hidden representations (Valeriani et al., 2023; Gurnee and Tegmark, 2024) and trajectory-level analyses of long-CoT reasoning (Jiang et al., 2025), we use sentence-boundary hidden states as an operational proxy for reasoning-state evolution. Specifically, hidden displacement measures the magnitude of representation change between consecutive reasoning steps, while forward progress measures the component of this change aligned with the terminal direction of the analyzed trace. These metrics characterize representation-level state movement and terminal-directional progress under an operational proxy. Because the terminal direction is derived from the observed trace representation, forward progress should be interpreted as an operational terminal-directional proxy rather than a ground-truth answer direction. We further compute progress efficiency, defined as the ratio between forward progress and hidden displacement, to measure how effectively local state movement is converted into directional

progress. To control for sentence length, we also report token-normalized variants of hidden displacement and forward progress. Curvature is included as an auxiliary diagnostic of directional change, while displacement, forward progress, and efficiency serve as the primary geometric indicators. The detailed protocols are described in Appendix.

Distributional geometric tendency. Figure 3(a) shows that many sentences in both groups have near-zero token-normalized hidden displacement, suggesting that fine-grained geometric scores should not be used as hard sentence-level deletion criteria. Nevertheless, retained reasoning is shifted toward larger displacement, indicating stronger state movement per token than editor-removed continuation. Figure 3(b) shows a similar pattern. Although the two groups overlap substantially in the scatter space, retained reasoning more often exhibits larger hidden displacement and stronger forward progress. Thus, geometry provides a distributional signal of useful reasoning progress rather than a pointwise separation rule.

Paired evidence. Table 1 gives a paired per-sample comparison and shows that editor-removed continuation has weaker operational hidden-state progress than retained reasoning. For hidden displacement, the removed mean is much lower than the retained mean (21.91 vs. 44.92), and the paired difference is consistently negative, with 79% of samples showing lower values for the removed segment. Forward progress shows the same trend, suggesting that the removed continuation advances less under the terminal-directional proxy. These gaps remain after token normalization, where both hidden displacement per token and forward progress per token are lower for editor-removed continuation. By contrast, curvature has only a small absolute gap, suggesting that the post-conclusion continuation is associated mainly with weaker displacement and weaker terminal-directional progress, rather than with a curvature pattern.

3.4 Uncertainty–Geometry Mismatch

The above analyses reveal a consistent diagnostic pattern in the editor-identified post-conclusion continuation. From the uncertainty view, this suffix often remains locally costly or unstable, while evaluator-based answer recoverability no longer improves consistently. From the geometric view, the same suffix shows weaker hidden displacement and weaker terminal-directional progress than retained reasoning. We refer to this pattern as an uncertainty–geometry mismatch. Importantly, this mismatch is not used to define harmfulness and does not by itself prove causal training harm. Instead, it characterizes the editor-removable post-conclusion continuation that is later tested through downstream SFT intervention.

4 Method

Our diagnostic analysis suggests that editor-removed post-conclusion continuation is associated with persistent local uncertainty and weak terminal-directional hidden-state progress. Based on this operational pattern, we instantiate a lightweight boundary proxy termed Harmful Continuation Cut.

4.1 Boundary Proxy

Given a question q and a verified source trajectory, we separate the sentence-level reasoning trace from the final answer. Let $r = (r_1, r_2, \dots, r_T)$ denote the reasoning trace, and let a^* denote the final answer. Let $c^* \in \{0, \dots, T\}$ denote the editor-identified post-conclusion continuation boundary used for supervision. Our goal is to learn a lightweight proxy that predicts this boundary, so that the retained prefix $r_{\leq c^*}$ is kept while the post-conclusion continuation $r_{> c^*}$ is removed.

We encode the question and reasoning trace with a frozen causal language model and extract a hidden representation at each sentence boundary, obtaining $h_t \in \mathbb{R}^D$. This representation denotes the model state after consuming the prefix up to sentence r_t . We then pass the sentence-level states through a shared sequence encoder:

$$\tilde{h}_t = \text{SeqEnc}(h_{1:T})_t. \quad (1)$$

The contextualized representation \tilde{h}_t is used as the common input for latent regularization and uncertainty–geometry diagnostic estimation.

4.2 Sequential Latent Regularization

HCC uses a sequential variational latent representation to regularize sentence-level boundary states.

For each contextualized sentence state \tilde{h}_t , we define a posterior latent distribution:

$$q_\phi(z_t | \tilde{h}_t) = \mathcal{N}(\mu_t, \Sigma_t), \quad (2)$$

where the mean and variance are predicted from \tilde{h}_t . We also define a sequential prior from the previous contextual state:

$$p_\eta(z_t | h_{t-1}) = \mathcal{N}(\mu_t^p, \Sigma_t^p). \quad (3)$$

The sampled latent variable is projected back to the boundary-prediction space:

$$b_t = f_{\text{lat}}(z_t). \quad (4)$$

The latent representation is regularized by:

$$\mathcal{L}_{\text{KL}} = \sum_{t=1}^T D_{\text{KL}}(q_\phi(z_t | \tilde{h}_t) \| p_\eta(z_t | h_{t-1})). \quad (5)$$

This term provides compact latent regularization for boundary prediction, rather than a hard information bottleneck or an explicit answer-prediction objective.

4.3 Uncertainty–Geometry Diagnostic Estimation

Post-conclusion continuation may remain locally costly or unstable while contributing limited hidden-state progress. To capture this uncertainty–geometry mismatch, HCC jointly estimates a local uncertainty signal and an operational progress signal from h_t .

For uncertainty, we define a scalar target T_t from source-trace sentence-level statistics such as entropy, NLL, or log-perplexity. HCC estimates this signal as:

$$s_t^{\text{ent}}, \hat{T}_t = f_{\text{ent}}(\tilde{h}_t), \quad (6)$$

where s_t^{ent} is the uncertainty-aware context vector used for boundary prediction, and \hat{T}_t is the scalar uncertainty estimate. The regression loss is:

$$\mathcal{L}_{\text{ent}} = \sum_{t=1}^T \text{Huber}(\hat{T}_t, T_t). \quad (7)$$

For geometry, we define a scalar progress target G_t from hidden-state movement statistics. HCC estimates this signal as:

$$s_t^{\text{geo}}, \hat{G}_t = f_{\text{geo}}(\tilde{h}_t), \quad (8)$$

where s_t^{geo} is the progress-aware context vector used for boundary prediction, and \hat{G}_t is the scalar progress estimate. The regression loss is:

$$\mathcal{L}_{\text{geo}} = \sum_{t=1}^T \text{Huber}(\hat{G}_t, G_t). \quad (9)$$

Together, these estimates provide a unified diagnostic representation of whether a post-conclusion sentence remains locally uncertain while showing weak operational progress.

4.4 Mismatch-Aware Boundary Prediction

HCC fuses the latent regularization signal with the uncertainty–geometry diagnostic representation in a shared boundary-prediction space:

$$m_t = \text{LN}(b_t + \alpha_{\text{geo}} s_t^{\text{geo}} + \alpha_{\text{ent}} s_t^{\text{ent}}), \quad (10)$$

where α_{geo} and α_{ent} are learnable scalar gates. Thus, HCC does not concatenate the raw contextual state directly into the final cut representation. Instead, the scalar estimates \hat{T}_t and \hat{G}_t are trained with auxiliary losses, while their context vectors contribute to boundary prediction.

For cut prediction, we prepend a learned beginning-of-sequence state m_0 and compute:

$$\pi_t = \text{CutHead}(m_t), \quad t = 0, \dots, T. \quad (11)$$

Here, π_t denotes the logit of choosing sentence t as the last retained sentence. Given the editor-identified boundary c^* , the cut head is trained with:

$$\mathcal{L}_{\text{cut}} = -\log \frac{\exp(\pi_{c^*})}{\sum_{j=0}^T \exp(\pi_j)}. \quad (12)$$

We also train a sentence-level deletion head to match the deletion labels produced by the offline editor. Let $y_t \in \{0, 1\}$ denote whether sentence r_t should be deleted. The deletion probability is:

$$\hat{y}_t = \text{DelHead}(m_t), \quad (13)$$

with the binary deletion loss:

$$\mathcal{L}_{\text{del}} = -\sum_{t=1}^T [y_t \log \hat{y}_t + (1 - y_t) \log(1 - \hat{y}_t)]. \quad (14)$$

The overall training objective is:

$$\mathcal{L} = \mathcal{L}_{\text{cut}} + \lambda_{\text{del}} \mathcal{L}_{\text{del}} + \lambda_{\text{KL}} \mathcal{L}_{\text{KL}} + \lambda_{\text{ent}} \mathcal{L}_{\text{ent}} + \lambda_{\text{geo}} \mathcal{L}_{\text{geo}}. \quad (15)$$

5 Experiments

5.1 Experimental Setup

Datasets. We use the same trajectories as in Section 3, also denoted as $\{T\}_Q$ and $\{T\}_R$. For HCC training, we use the 500M-scale Qwen2.5-0.5B-Instruct as a frozen backbone and train lightweight prediction heads to learn the

editor-identified removable post-conclusion continuation boundary. To test whether the learned deletion rule transfers across nearby source-model families rather than only memorizing a single source style, we construct the train–validation split across source models. Specifically, we use $\{T\}_Q$ to train HCC, then process $\{T\}_R$ with the trained HCC and SFT the baseline model on the processed $\{T\}_R$, and vice versa.

Evaluation metrics. As for the comparison methods, we include 4 different methods to process the original trajectories, including (1) Vanilla, indicating that the original trajectories are directly used for SFT without any processing; (2) Editor, indicating that the trajectory is processed by Qwen3.5-27B to remove the post-conclusion continuation; (3) Heuristic, indicating the heuristic method proposed by (Li et al., 2026) and (4) HCC, indicating the proposed method in this paper. We evaluate the resulting SFT models on three reasoning benchmarks: MATH500, AMC23, and GSM8K. The primary evaluation metric is pass@1.

5.2 Main Results

Overall comparisons. Table 2 reports the main SFT results using different processed versions of the same answer-correct long-CoT traces. From the results, we can draw several conclusions: (1) Across different training traces and models, answer-preserving removal of the editor-identified post-conclusion continuation improves downstream SFT outcomes over training on the original traces. This provides interventional evidence that the post-conclusion continuation is training-unfavorable in these settings. (2) HCC achieves performance close to the 27B editor-processed reference, and in several cases even surpasses it. For example, in the LLaMA3.2-3B setting, HCC obtains an average score of 45.2 on $\{T\}_Q$ and 49.3 on $\{T\}_R$, closely matching the editor-processed results of 45.7 and 49.8. HCC also outperforms the editor reference on MATH500 under $\{T\}_Q$ and on GSM8K under $\{T\}_R$. These results indicate that a lightweight boundary proxy can recover much of the benefit of large-model delete-only trace editing. (3) Compared with heuristic truncation, HCC-processed traces are both more accurate and substantially shorter in response length. The comparison with heuristic truncation suggests that length reduction alone may not fully explain the gains, although length-controlled interventions would be needed for a complete separation.

Table 2: Main results using different long-CoT trajectories. Len. denotes the average response length.

Method	SFT on $\{T\}_Q$					SFT on $\{T\}_R$				
	MATH500	AMC23	GSM8K	Avg.	Len.	MATH500	AMC23	GSM8K	Avg.	Len.
Backbone: LLaMA3.2-3B-Instruct										
Vanilla	29.8	10.0	69.0	36.3	3478.8	38.4	15.0	69.9	41.1	4967.1
Heuristic	34.0	15.0	71.5	40.2	3430.8	40.0	15.0	70.1	41.7	5172.1
Editor	<u>41.8</u>	20.0	75.4	45.7	1906.1	51.2	22.5	<u>75.9</u>	49.8	1942.1
HCC	43.2	<u>17.5</u>	<u>75.1</u>	<u>45.2</u>	2010.1	<u>47.6</u>	22.5	77.8	<u>49.3</u>	1934.4
Backbone: Qwen2.5-Math-7B-Instruct										
Vanilla	85.8	<u>62.5</u>	95.8	81.4	519.6	85.6	62.5	95.8	81.3	510.6
Heuristic	82.8	<u>57.5</u>	95.8	78.7	526.1	84.4	62.5	95.7	80.9	498.5
Editor	<u>84.4</u>	70.0	96.2	83.5	499.0	<u>86.4</u>	67.5	<u>96.0</u>	83.3	443.2
HCC	82.6	<u>62.5</u>	<u>96.1</u>	80.4	497.9	86.6	<u>65.0</u>	96.2	<u>82.6</u>	455.9

5.3 More Experiments

Analysis of uncertainty dynamics. Figure 4 compares the reasoning dynamics of models trained on original, HCC-processed, and editor-processed traces. In Figure 4 (a), Vanilla shows a sharp late-stage increase in answer NLL, suggesting that generated reasoning becomes less favorable under evaluator-based answer recoverability. In contrast, both HCC and Editor keep answer NLL much more stable across the reasoning process, suggesting that post-conclusion continuation removal improves answer-support consistency under this diagnostic. Figure 4 (b) further shows the segment-level uncertainty pattern. Vanilla first reduces entropy but then exhibits a clear entropy rebound in the later reasoning bins, which is consistent with re-entering an unstable post-conclusion continuation. By comparison, HCC and Editor continue to reduce segment entropy in the later stage and produce highly similar curves. These curves provide post-training diagnostic evidence consistent with Section 3 pattern. The similarity between HCC and Editor curves suggests that the lightweight proxy approximates the diagnostic behavior of delete-only edited traces.

Analysis of geometric dynamics. Figure 5 examines whether processed traces lead to stronger hidden-state progress under the chosen proxy. In Figure 5 (a), HCC and Editor produce larger token-normalized hidden displacement than Vanilla, suggesting stronger state movement per generated token. Figure 5 (b) shows that Vanilla exhibits a clearer positive entropy-progress mismatch in the middle and late stages, where uncertainty is not matched by sufficient geometric progress. By contrast, HCC and Editor keep this mismatch closer to

zero and reduce it near the end. These curves provide post-training diagnostic evidence consistent with Section 3 pattern, and again suggest that HCC approximates the delete-only editor behavior.

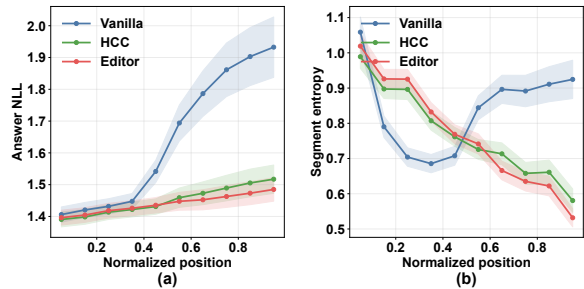


Figure 4: Post-training uncertainty diagnostics for generated reasoning traces.

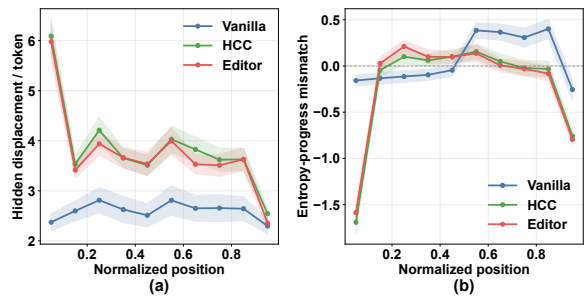


Figure 5: Operational uncertainty-progress diagnostics in generated reasoning traces.

Analysis of reinforcement learning. We further examine whether HCC-processed SFT provides a stronger initialization for subsequent GRPO training. Using LLaMA3.2-3B-Instruct trained on $\{T\}_Q$, we apply GRPO to the checkpoints obtained from Vanilla SFT and HCC-based SFT, and evaluate performance across different RL steps. As shown in Table 3, the model initialized from HCC-based SFT consistently outperforms the Vanilla

counterpart at each evaluated step. The model initialized from HCC-based SFT maintains higher performance across the evaluated RL steps in this setting. This suggests that harmful continuation removal can provide a stronger SFT initialization. More broadly, the effect of SFT data processing can persist into subsequent RL.

Table 3: Comparison across reinforcement steps.

Method	Dataset	0	10	20	30	40
Vanilla	MATH500	29.8	34.8	35.2	36.6	36.4
	GSM8K	69.0	71.6	72.7	73.1	73.3
HCC	MATH500	43.2	45.8	46.0	46.2	49.4
	GSM8K	75.1	75.4	75.7	77.7	77.0

Table 4: Comparison of random cut and HCC-based method on LLaMA3.2-3B-Instruct.

Method	MATH500	AMC23	GSM8K	Avg.
Random Cut	31.4	7.5	48.1	29.0
HCC	47.6	22.5	77.8	49.3

Analysis of Random Cut. We further introduce a random cut baseline to rule out the possibility that the improvement mainly comes from shorter responses. To align it with HCC, random cut preserves the final answer, removes a sentence-complete suffix from the reasoning trace, and controls the removed length to match the average truncation length of HCC. As shown in Table 4, random cut is consistently inferior to HCC on MATH500, AMC23, and GSM8K, yielding an average score of only 29.0 compared with 49.3 for HCC. This large gap suggests that arbitrary length reduction is not a reliable solution. Since random cut does not identify whether the reasoning has already concluded, it may discard necessary intermediate steps and damage the reasoning chain. HCC instead removes post-conclusion continuation, thereby reducing redundant tail reasoning while preserving the core answer-supporting process.

Analysis of MMLU datasets. We further examine whether the SFT improvements transfer to several non-mathematical evaluation subjects on MMLU (Hendrycks et al., 2021). As shown in Figure 6, we select 6 subjects that require different types of knowledge, including college physics, college biology, clinical knowledge, professional psychology, high school statistics, and high school biology. From the results, we can see that HCC-

based SFT outperforms Vanilla-based SFT across all subjects, and achieves comparable performance to the editor-based reference. These results suggest that models trained on HCC-processed mathematical traces can retain or improve performance on selected out-of-domain knowledge-intensive evaluations. They do not by themselves establish that the same harmful continuation pattern appears in non-mathematical training traces. The overall performance of different models and different SFT data settings are shown in the Appendix.

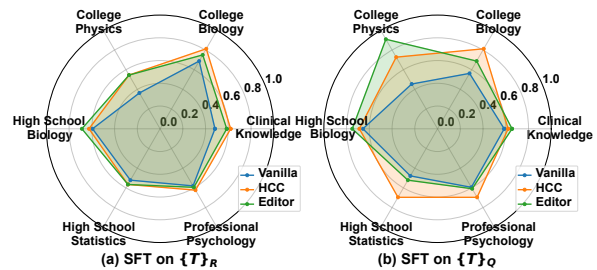


Figure 6: Visualization of the performance of LLaMA3.2-3B-Instruct on selected MMLU subjects.

6 Conclusion

We studied post-conclusion continuation in answer-correct long-CoT SFT traces, where generation continues after the answer appears sufficiently supported. Using a delete-only editor, we constructed answer-preserving post-conclusion continuation removal and observed improved downstream SFT outcomes, suggesting that the removed continuation is training-unfavorable in our setting. We therefore refer to this empirically supported phenomenon as harmful continuation. We further characterized the removed continuation through uncertainty and operational hidden-state analyses, revealing an uncertainty–geometry mismatch. Based on this, we instantiated HCC as a lightweight boundary proxy for approximating editor-identified post-conclusion continuation removal.

Limitations

The delete-only editor provides an operational intervention, not a ground-truth oracle of harmfulness; its labels should be understood as editor-identified post-conclusion continuation boundaries. Our measurements are diagnostic proxies rather than causal proof of training harm. Finally, HCC approximates the editor-identified removal boundary rather than intrinsic harmfulness, and finer component-level attribution remains future work.

References

- Marthe Ballon, Brecht Verbeken, Vincent Ginis, and Andres Algaba. 2026. Probing the trajectories of reasoning traces in large language models. *arXiv preprint arXiv:2601.23163*.
- Paul C Bogdan, Uzay Macar, Neel Nanda, and Arthur Conmy. Thought anchors: Which llm reasoning steps matter? In *Mechanistic Interpretability Workshop at NeurIPS 2025*.
- Abhranil Chandra, Ayush Agrawal, Arian Hosseini, Sebastian Fischmeister, Rishabh Agarwal, Navin Goyal, and Aaron Courville. 2025. Shape of thought: When distribution matters more than correctness in reasoning tasks. *arXiv preprint arXiv:2512.22255*.
- Wei-Rui Chen, Vignesh Kothapalli, Ata Fatahbaazri, Hejian Sang, Shao Tang, Qingquan Song, Zhipeng Wang, and Muhammad Abdul-Mageed. 2025a. Distilling the essence: Efficient reasoning distillation via sequence truncation. *arXiv preprint arXiv:2512.21002*.
- Xingyu Chen, Jiahao Xu, Tian Liang, Zhiwei He, Jianhui Pang, Dian Yu, Linfeng Song, Qiuzhi Liu, Mengfei Zhou, Zhuosheng Zhang, and 1 others. 2025b. Do not think that much for $2+3=?$ on the overthinking of long reasoning models. In *Forty-second International Conference on Machine Learning*.
- Daya Guo, Dejian Yang, Haowei Zhang, Junxiao Song, Peiyi Wang, Qihao Zhu, Runxin Xu, Ruoyu Zhang, Shirong Ma, Xiao Bi, and 1 others. 2025. Deepseek-r1 incentivizes reasoning in llms through reinforcement learning. *Nature*, 645(8081):633–638.
- Wes Gurnee and Max Tegmark. 2024. Language models represent space and time. In *International Conference on Learning Representations*, volume 2024, pages 2483–2503.
- Dan Hendrycks, Collin Burns, Steven Basart, Andy Zou, Mantas Mazeika, Dawn Song, and Jacob Steinhardt. 2021. Measuring massive multitask language understanding. *Proceedings of the International Conference on Learning Representations (ICLR)*.
- Gangwei Jiang, Yahui Liu, Zhaoyi Li, Wei Bi, Fuzheng Zhang, Linqi Song, Ying Wei, and Defu Lian. 2025. What makes a good reasoning chain? uncovering structural patterns in long chain-of-thought reasoning. In *Proceedings of the 2025 Conference on Empirical Methods in Natural Language Processing*, pages 6501–6525.
- Yuetai Li, Xiang Yue, Zhangchen Xu, Fengqing Jiang, Luyao Niu, Bill Yuchen Lin, Bhaskar Ramasubramanian, and Radha Poovendran. 2025. Small models struggle to learn from strong reasoners. In *Findings of the Association for Computational Linguistics: ACL 2025*, pages 25366–25394.
- Zhaoyi Li, Xiangyu Xi, Zhengyu Chen, Wei Wang, Gangwei Jiang, Ranran Shen, Linqi Song, Ying Wei, and Defu Lian. 2026. On the role of reasoning patterns in the generalization discrepancy of long chain-of-thought supervised fine-tuning. *arXiv preprint arXiv:2604.01702*.
- Zhenghao Liu, Zhuoyang Wu, Xinze Li, Yukun Yan, Shuo Wang, Zulong Chen, Yu Gu, Ge Yu, and Maosong Sun. 2026. Long-chain reasoning distillation via adaptive prefix alignment. *arXiv preprint arXiv:2601.10064*.
- Haotian Luo, Li Shen, Haiying He, Yibo Wang, Shiwei Liu, Wei Li, Naiqiang Tan, Xiaochun Cao, and Dacheng Tao. 2025a. O1-pruner: Length-harmonizing fine-tuning for o1-like reasoning pruning. *arXiv preprint arXiv:2501.12570*.
- Yijia Luo, Yulin Song, Xingyao Zhang, Jiaheng Liu, Weixun Wang, GengRu Chen, Wenbo Su, and Bo Zheng. 2025b. Deconstructing long chain-of-thought: A structured reasoning optimization framework for long cot distillation. *arXiv preprint arXiv:2503.16385*.
- Xinyin Ma, Guangnian Wan, Runpeng Yu, Gongfan Fang, and Xinchao Wang. 2025. Cot-valve: Length-compressible chain-of-thought tuning. In *Proceedings of the 63rd Annual Meeting of the Association for Computational Linguistics (Volume 1: Long Papers)*, pages 6025–6035.
- Linyu Ou and YuYang Yin. 2025. Empowering lightweight mllms with reasoning via long cot sft. *arXiv preprint arXiv:2509.03321*.
- Gianluigi Silvestri and Edoardo Cetin. 2026. Learning from partial chain-of-thought via truncated-reasoning self-distillation. *arXiv preprint arXiv:2603.13274*.
- Yiliu Sun, Zicheng Zhao, Yang Wei, Yanfang Zhang, and Chen Gong. 2026. Well begun, half done: Reinforcement learning with prefix optimization for llm reasoning. In *Proceedings of the AAAI Conference on Artificial Intelligence*, volume 40, pages 33144–33152.
- Qwen Team. 2025. [Qwen3 technical report](#). *Preprint*, arXiv:2505.09388.
- Xiaoyu Tian, Yunjie Ji, Haotian Wang, Shuaiting Chen, Sitong Zhao, Yiping Peng, Han Zhao, and Xiang-gang Li. 2025. Not all correct answers are equal: Why your distillation source matters. *arXiv preprint arXiv:2505.14464*.
- Lucrezia Valeriani, Diego Doimo, Francesca Cuturello, Alessandro Laio, Alessio Ansuini, and Alberto Cazzaniga. 2023. The geometry of hidden representations of large transformer models. *Advances in Neural Information Processing Systems*, 36:51234–51252.

- Shenzhi Wang, Le Yu, Chang Gao, Chujie Zheng, Shixuan Liu, Rui Lu, Kai Dang, Xiong-Hui Chen, Jianxin Yang, Zhenru Zhang, and 1 others. 2026. Beyond the 80/20 rule: High-entropy minority tokens drive effective reinforcement learning for llm reasoning. *Advances in Neural Information Processing Systems*, 38:115452–115486.
- Jason Wei, Xuezhi Wang, Dale Schuurmans, Maarten Bosma, Fei Xia, Ed Chi, Quoc V Le, Denny Zhou, and 1 others. 2022. Chain-of-thought prompting elicits reasoning in large language models. *Advances in neural information processing systems*, 35:24824–24837.
- Silei Xu, Wenhao Xie, Lingxiao Zhao, and Pengcheng He. 2025. Chain of draft: Thinking faster by writing less. *arXiv preprint arXiv:2502.18600*.
- Shiming Yang, Yuxuan Tong, Xinyao Niu, Graham Neubig, and Xiang Yue. 2025. Demystifying long chain-of-thought reasoning. In *Forty-second International Conference on Machine Learning*.
- Yuming Yang, Mingyoung Lai, Wanxu Zhao, Xiaoran Fan, Zhiheng Xi, Mingqi Wu, Chiyue Huang, Jun Zhao, Haijun Lv, Jian Tong, and 1 others. 2026. Which reasoning trajectories teach students to reason better? a simple metric of informative alignment. *arXiv preprint arXiv:2601.14249*.
- Dylan Zhang, Qirun Dai, and Hao Peng. 2025. The best instruction-tuning data are those that fit. *arXiv preprint arXiv:2502.04194*.

A Implementation Details

We implement SFT with LLaMAFactory. All models are fine-tuned with the AdamW optimizer using a learning rate of 1×10^{-5} . For fair comparison, Vanilla, Heuristic, Editor, and HCC use the same training configuration, and only differ in the SFT traces used for supervision. During evaluation, we fix the decoding temperature to 0 to ensure deterministic generation and improve reproducibility. All benchmark results are reported under this fixed evaluation setting.

B Information Bottleneck Motivation for Answer-Sufficiency

In this appendix, we provide an information-bottleneck motivation for the answer-sufficiency component of HCC. The goal is to formalize when a reasoning prefix can already support the final answer, and to give an idealized sufficient condition under which a suffix does not change the answer decision under an answer-prediction head.

B.1 Sequential Conditional Information Bottleneck

Given a question Q , a sentence-level reasoning trace $R = (r_1, \dots, r_T)$, and the final answer A , let $R_{\leq t}$ and $R_{> t}$ denote the prefix and suffix at step t . For each prefix $R_{\leq t}$, we introduce a stochastic bottleneck representation Z_t induced from the contextualized reasoning state \tilde{h}_t :

$$q_\phi(z_t | \tilde{h}_t) = \mathcal{N}(\mu_t, \Sigma_t).$$

The ideal conditional information bottleneck objective aims to preserve answer-relevant information while removing unnecessary dependence on the reasoning prefix:

$$\begin{aligned} \min \quad & I(Z_t; R_{\leq t} | Q) \\ \text{s.t.} \quad & I(Z_t; A | Q) \text{ is sufficiently large.} \end{aligned}$$

Equivalently, one may optimize the following Lagrangian form:

$$\mathcal{J}_{\text{IB}} = -I(Z_t; A | Q) + \beta I(Z_t; R_{\leq t} | Q).$$

Since exact mutual information is intractable for free-form reasoning traces, we use a variational approximation. The answer-relevance term is optimized through a variational answer predictor $p_\psi(a | z_t, q)$, leading to the negative log-likelihood term:

$$-\log p_\psi(a^* | z_t, q).$$

For the compression term, we introduce a sequential prior $p_\eta(z_t | z_{t-1}, q)$ and use the following KL penalty as a variational surrogate for the incremental information injected into the bottleneck:

$$D_{\text{KL}}(q_\phi(z_t | \tilde{h}_t) \| p_\eta(z_t | z_{t-1}, q)).$$

Thus, the practical sequential IB loss is:

$$\mathcal{L}_{\text{IB}} = \sum_{t=1}^T \left[-\log p_\psi(a^* | z_t, q) + \beta D_{\text{KL}}(q_\phi(z_t | \tilde{h}_t) \| p_\eta(z_t | z_{t-1}, q)) \right].$$

This objective encourages Z_t to retain information predictive of the final answer while discouraging unnecessary state complexity.

B.2 Ideal Answer-Sufficiency Boundary

We next formalize an ideal boundary after which the remaining reasoning suffix provides no additional answer information under the bottleneck representation.

Definition. The ideal answer-sufficiency boundary is defined as:

$$\tau^* = \min \{t : I(A; R_{>t} | Q, Z_t) = 0\}.$$

This condition means that, once Q and Z_t are given, the suffix $R_{>t}$ provides no additional information about the final answer A . If the set is empty, the trace has no boundary satisfying this ideal condition.

Proposition. If

$$I(A; R_{>t} | Q, Z_t) = 0,$$

then conditioning on $R_{>t}$ does not change the Bayes-optimal answer distribution given (Q, Z_t) .

Proof. By the definition of conditional mutual information, the condition

$$I(A; R_{>t} | Q, Z_t) = 0$$

implies the conditional independence relation:

$$A \perp R_{>t} | (Q, Z_t).$$

Therefore, for any answer candidate a , we have:

$$p(a | Q, Z_t, R_{>t}) = p(a | Q, Z_t).$$

As a result, the Bayes-optimal answer predictor satisfies:

$$\arg \max_a p(a | Q, Z_t, R_{>t}) = \arg \max_a p(a | Q, Z_t).$$

Thus, once Z_t is answer-sufficient in the conditional-independence sense, the suffix $R_{>t}$ is irrelevant to the answer decision under the bottleneck representation. \square

Remark. This proposition establishes an answer-sufficiency condition only. It does not imply that deletion necessarily improves SFT. The empirical benefit studied in the main paper additionally depends on whether the answer-sufficient suffix introduces high local uncertainty or weak geometric progress as supervision.

C Experimental Settings

C.1 Uncertainty Metrics

We compute uncertainty metrics with a fixed evaluator model. Each answer-correct trace is split into sentence-level units, and the final boxed answer is used as the answer target. When scoring intermediate reasoning text, standalone boxed-answer strings are removed to reduce trivial answer leakage.

For sentence-level uncertainty, each sentence $r_t = (y_1, \dots, y_m)$ is scored under its preceding context P_{t-1} . We report token-averaged NLL and predictive entropy:

$$\text{NLL}_{\text{sent}}(r_t) = -\frac{1}{m} \sum_{i=1}^m \log p(y_i | P_{t-1}, y_{<i}),$$

$$\text{Ent}_{\text{sent}}(r_t) = \frac{1}{m} \sum_{i=1}^m H(p(\cdot | P_{t-1}, y_{<i})).$$

For answer-level uncertainty, we measure how a reasoning prefix affects recovery of the boxed answer $a^* = (a_1, \dots, a_L)$. Given the prefix P_t after appending sentence r_t , we compute:

$$\text{NLL}_{\text{ans}}(P_t) = -\frac{1}{L} \sum_{i=1}^L \log p(a_i | P_t, a_{<i}).$$

Answer entropy is computed analogously over the answer-token positions. We define answer-NLL reduction as:

$$\Delta_{\text{ans}}(t) = \text{NLL}_{\text{ans}}(P_{t-1}) - \text{NLL}_{\text{ans}}(P_t).$$

A larger value means that appending r_t makes the final answer easier to recover under the evaluator.

For segment-wise plots, sentences are appended along the original complete trace, while the x-axis is normalized separately within retained reasoning and editor-removed continuation. For boundary-level plots, K_1 and K_T denote the first and last retained sentences, and C_1 and C_T denote the first and last editor-removed sentences.

C.2 Geometric Metrics

We compute geometric metrics from hidden states at sentence boundaries. Let h_t denote the evaluator hidden state after consuming the prefix ending at sentence r_t . The local state update is:

$$\Delta h_t = h_t - h_{t-1}.$$

Hidden displacement measures the size of this update:

$$D_t = \|\Delta h_t\|_2.$$

Forward progress measures the projection of the local update onto the remaining direction toward the terminal state of the analyzed trace:

$$G_t = \frac{\langle \Delta h_t, h_T - h_{t-1} \rangle}{\|h_T - h_{t-1}\|_2 + \epsilon}.$$

This is an operational proxy for terminal-directional hidden-state progress, not a direct measurement of the true reasoning process.

Progress efficiency is defined as:

$$E_t = \frac{G_t}{D_t + \epsilon}.$$

To control for sentence length, we also report token-normalized variants:

$$D_t^{\text{tok}} = \frac{D_t}{n_t}, \quad G_t^{\text{tok}} = \frac{G_t}{n_t},$$

where n_t is the token length of r_t .

Curvature is used only as an auxiliary direction-change diagnostic:

$$\text{Curv}_t = 1 - \frac{\langle \Delta h_{t-1}, \Delta h_t \rangle}{\|\Delta h_{t-1}\|_2 \|\Delta h_t\|_2 + \epsilon}, \quad t > 1.$$

For paired comparisons, we average each metric within retained reasoning and editor-removed continuation for each example. The paired difference is:

$$\Delta = \text{Mean}_{\text{removed}} - \text{Mean}_{\text{retained}}.$$

We report group means, the fraction of examples where the removed continuation is lower or higher, and the 95% confidence interval of Δ .

D Additional Experiments

D.1 Additional Analysis of Harmful Continuation Diagnostics

Uncertainty View. Figure 7 compares the answer-level perturbation induced by retained reasoning and editor-removed continuation. Editor-removed continuation shows larger NLL perturbation and a right-shifted distribution of average log-probability perturbation. This suggests that the removed harmful continuation is not simply irrelevant text, but remains answer-conditioned and introduces stronger instability to evaluator-based final-answer prediction.

Geometric View. Figure 8 further compares the geometric behavior of the two groups. Retained reasoning induces larger token-normalized hidden displacement, while editor-removed continuation is more concentrated in the low forward-progress region. This is consistent with the view that editor-removed continuation corresponds to a low-progress phase: it can still affect answer prediction, but does not provide comparable representation-level state movement toward the terminal reasoning state. Together, these additional results support the uncertainty–geometry mismatch diagnosis of harmful continuation.

Table 5: Comparison of different methods across backbone models on the MMLU dataset. $\{T\}_Q$ and $\{T\}_R$ denote SFT trajectories from Qwen-style and R1-style long-CoT sources, respectively.

Method	LLaMA3.2-3B-Instruct		Qwen3-30B-A3B-Thinking-2507	
	$\{T\}_Q$	$\{T\}_R$	$\{T\}_Q$	$\{T\}_R$
Vanilla	60.1	58.0	85.4	84.6
Heuristic	59.8	60.1	85.0	85.3
Editor	61.1	60.6	85.2	85.4
HCC	62.9	60.8	85.7	85.7

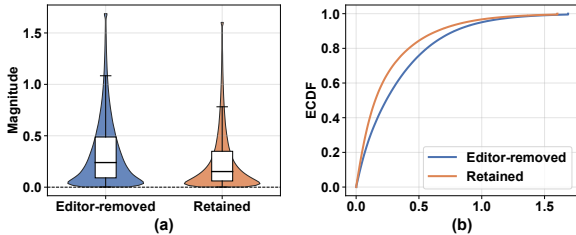


Figure 7: Additional uncertainty-side diagnosis. (a) NLL perturbation induced by retained reasoning and editor-removed continuation. (b) ECDF of average log-probability perturbation. Editor-removed continuation induces larger answer-level perturbations.

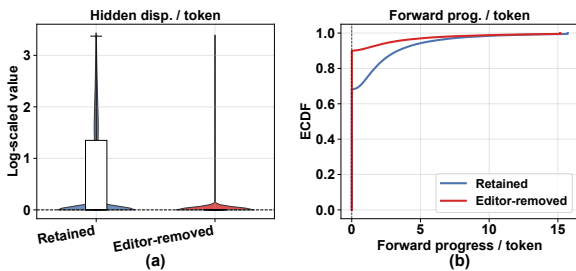


Figure 8: Additional geometry-side diagnosis. (a) Token-normalized hidden displacement of retained reasoning and editor-removed continuation. (b) ECDF of token-normalized forward progress. Editor-removed continuation is more concentrated in low-progress regions under the operational proxy.

D.2 Additional analysis of Test Datasets

Case study. Figure 9 presents a qualitative example comparing the same base model trained with HCC-processed traces and original long-CoT traces. The HCC-trained model quickly identifies the correct reasoning path, computes the remaining distance, and outputs the correct solution without entering a long verification loop. In contrast, the Vanilla-trained model first reaches the correct answer, but then derives a conflicting result from an alternative calculation, as shown in the gray region. After this conflict appears, the model repeatedly compares the two answers and rechecks different parts of the solution, entering a low-efficiency rea-

Table 6: HCC-based self-consistency diagnostics. Phase, Sent. ratio, and Len. denote the occurrence rate of outputs matching the HCC removable-continuation pattern, the corresponding sentence-level ratio, and the average token length, respectively. These metrics are detector-based consistency measures rather than independent evidence of harmfulness.

Dataset	Method	Phase ↓	Sent. ratio ↓	Len.
GSM8K	Vanilla	81.73	51.84	94.54
	Heuristic	93.63	59.91	96.19
	Editor	63.53	24.14	50.85
	HCC	60.42	19.45	48.38
MATH500	Vanilla	93.40	59.51	74.75
	Heuristic	93.60	60.06	73.99
	Editor	63.60	28.53	73.89
	HCC	61.80	27.35	66.86

soning loop highlighted in yellow. The response eventually exhausts the token budget without producing a successful final answer. This example qualitatively illustrates a behavior consistent with the harmful continuation pattern: the model may continue uncertain, low-progress verification even after a sufficient answer has already been reached. It suggests that HCC-processed supervision can reduce such continuation patterns.

HCC-based self-consistency diagnostic. Table 6 evaluates whether model outputs after SFT match the removable post-conclusion continuation pattern learned by HCC. For a fair cross-source test, we use the HCC proxy trained on $\{T\}_Q$ to analyze outputs from models trained on $\{T\}_R$ -based data. This analysis should be interpreted as a detector-based self-consistency diagnostic rather than an independent measurement of causal harmfulness. Under this diagnostic, models trained on HCC-processed traces produce fewer outputs that are classified as containing removable post-conclusion continuation. For example, HCC reduces the sentence-level detected continuation ratio from 51.84% to 19.45% on GSM8K and from 59.51% to 27.35% on MATH500.

Method	# Params	MACs	FLOPs	Rel. MACs
Qwen3.5-27B	27.0B	137.1T	274.3T	$\sim 54.2\times$
HCC	498.0M	2.5T	5.1T	$1.0\times$

Table 7: Computational cost comparison given similar input lengths of Qwen3.5-27B and HCC.

Analysis of Computational Costs. Table 7 compares the computational cost of the 27B offline editor and our HCC proxy given similar input lengths. HCC uses only 498M parameters, which is about 1.8% of Qwen3.5-27B. It also requires 2.5T MACs and 5.1T FLOPs, compared with 137.1T MACs and 274.3T FLOPs for Qwen3.5-27B. This corresponds to a roughly $54.2\times$ reduction in computation. These results show that HCC provides a much cheaper proxy for editor-identified harmful continuation boundary approximation, making large-scale SFT trace processing more practical.

Question: John drives for 3 hours at a speed of 60 mph and then turns around because he realizes he forgot something very important at home. He tries to get home in 4 hours but spends the first 2 hours in standstill traffic. He spends the next half-hour driving at a speed of 30mph, before being able to drive the remaining time of the 4 hours going at 80 mph. How far is he from home at the end of those 4 hours?

<think>Okay, let's try to figure out how far John is from home after all that. First, John drives for 3 hours at 60 mph. So, the distance he covers in that first part is speed multiplied by time, right? So 60 mph times 3 hours is 180 miles. That means he's 180 miles away from home when he turns around. Then, he wants to get home in 4 hours, but he's stuck in traffic for the first 2 hours. So, during those 2 hours, he doesn't move. That means he's still 180 miles away from home, but he hasn't moved. Then, after the traffic, he starts driving again. The problem says he spends the next half-hour driving at 30 mph. Hmm, half-hour is 0.5 hours. So, 0.5 hours at 30 mph. Let's calculate that. Distance is speed times time, so $30 * 0.5$ is 15 miles. So, he covers 15 miles during that half-hour. But wait, he was 180 miles away from home, and he drove 15 miles. So now he's $180 - 15 = 165$ miles away from home. Then, the remaining time is 4 hours minus the 2 hours stuck in traffic and the half-hour driving at 30 mph. So, $4 - 2.5$ hours = 1.5 hours left. He drives the remaining 1.5 hours at 80 mph. So, distance is $80 * 1.5$. Let's calculate that. $80 * 1$ is 80, $80 * 0.5$ is 40, so total $80 + 40 = 120$ miles. So, he covers 120 miles during the last part. But he was 165 miles away, so now he's $165 - 120 = 45$ miles from home.</think>

To determine how far John is from home after the 4-hour journey, we break down his trip into segments:

1. First 3 hours at 60 mph:
 - Distance covered: $(60 \text{ mph}) \times 3 \text{ hours} = 180 \text{ miles}$. He is 180 miles away from home.
2. Stuck in traffic for 2 hours:
 - No movement, so he remains 180 miles away from home.
3. Driving at 30 mph for 0.5 hours:
 - Distance covered: $(30 \text{ mph}) \times 0.5 \text{ hours} = 15 \text{ miles}$.
 - New distance from home: $(180 \text{ miles}) - 15 \text{ miles} = 165 \text{ miles}$.
4. Driving at 80 mph for the remaining 1.5 hours:
 - Distance covered: $(80 \text{ mph}) \times 1.5 \text{ hours} = 120 \text{ miles}$.
 - Final distance from home: $(165 \text{ miles}) - 120 \text{ miles} = 45 \text{ miles}$.

<think>...So, the distance he covers in 1.5 hours is $80 * 1.5 = 120$ miles. Therefore, the total distance from home is $195 + 120 = 315$ miles. Wait, but hold on. Let me double-check. Let me make sure I didn't make a mistake here. Let's verify each step again. First, the initial 3 hours at 60 mph: $60 * 3 = 180$ miles. Correct. Then, he's stuck in traffic for 2 hours, so no movement. So, still 180 miles away. Then, he drives 0.5 hours at 30 mph: $30 * 0.5 = 15$ miles. So, total distance from home is $180 + 15 = 195$. Then, he has $4 - 2 - 0.5 = 1.5$ hours left. So, 1.5 hours at 80 mph. $80 * 1.5 = 120$ miles. So, total distance is $195 + 120 = 315$. Hmm, that seems right. But let me think again. Maybe I should use the formula for distance. The total time is 4 hours, but he spends 2 hours in traffic, so he's moving for $4 - 2 = 2$ hours. Then, he drives 0.5 hours at 30 mph, so that's $0.5 * 30 = 15$ miles. Then, the remaining 2 hours at 80 mph. So, $2 * 80 = 160$ miles. So, total distance is $15 + 160 = 175$ miles from home. Wait, that's different from 315. Hmm, that's a discrepancy. So, which one is correct? Wait, maybe I made a mistake in the time calculation. Let me check again. Total time: 4 hours. He spends 2 hours in traffic, so he's moving for $4 - 2 = 2$ hours. Then, he drives 0.5 hours at 30 mph, so that's $0.5 * 30 = 15$ miles. Then, the remaining 2 hours at 80 mph. So, $2 * 80 = 160$ miles. So, total distance is $15 + 160 = 175$ miles from home. But earlier, I thought it was $195 + 120 = 315$. So, which is correct? Wait, maybe I need to use the formula for distance. Let's use the formula: distance = speed * time. So, the total time he's moving is 4 hours, but he's stuck in traffic for 2 hours, so he's moving for $4 - 2 = 2$ hours. Then, he drives 0.5 hours at 30 mph, so that's $0.5 * 30 = 15$ miles. Then, the remaining 2 hours at 80 mph, so $2 * 80 = 160$ miles. So, total distance is $15 + 160 = 175$ miles from home. But earlier, I thought it was $195 + 120 = 315$. So, which is correct? Wait, maybe I need to consider the total time. ... So, which is correct? Wait, maybe I made a mistake in the initial 3 hours at 60 mph. ...

Figure 9: Case study of harmful continuation after SFT. The left part indicates the reasoning process of a model trained on HCC-processed traces, while the right part shows the reasoning process of a model trained on original traces. We use grey and yellow highlights to indicate the conflicting reasoning and the inefficient reasoning loop, respectively.